MERIDIONAL VARIABILITY FROM LARGE-APERTURE RING DIAGRAMS

I. González Hernández[1], R. Komm[1], F. Hill[1], R. Howe[1], and T. Corbard[2]

[1]*National Solar Observatory, Tucson, AZ, USA, Email: irenegh@nso.edu, komm@nso.edu, hill@nso.edu, rhowe@nso.edu*

[2]*Observatoire de la Côte d'Azur, Nice, France, Email: thierry.corbard@obs-nice.fr*

ABSTRACT

Ring Diagram analysis, a local helioseismology technique, has proven very useful in order to study the solar subsurface velocity ows down to a depth of about $0.97R_{\odot}$ (Hill, 1988). The depth range is determined by the modes used in this type of analysis and thus depends on the size of the area analyzed. Extending the area allows us to detect lower l modes which penetrate deeper in the Sun. However, there is a compromise between the size of the patch and the validity of the plane wave approximation used by the technique. This paper presents the results of applying ring diagrams to $30°$ diameter patches over the solar surface in an attempt to reach deeper into the solar interior. Meridional ows are derived using this technique.

Key words: Ring Diagrams; Meridional Circulation; Helioseismology.

1. INTRODUCTION

In this work, we have applied Ring Diagram analyses to patches of $30°$ diameter over the solar surface as they crossed the solar central meridian. These patches are twice the size of the typically studied sections of $15°$ in diameter (Gonzalez Hernandez et al., 1999). A set of 15 overlapping sections centered at latitudes $0°$, $\pm 7.5°$, $\pm 15°$, $\pm 22.5°$,$\pm 30°$, $\pm 37.5°$,$\pm 45°$ and $\pm 52.5°$ have been analyzed for 25 intervals of 1664 minutes during Carrington rotations 1979, 1987, 1988, 1989, 1990, 1991 and 1992. These CRs span from 03/02/2002 to 08/12/2002. Most of the processing work has been done using the GONG Ring Diagram Pipeline (Corbard et al., 2003).

Fig. 1 shows a comparison between the set of modes in the range l=0-600 tted using a $15°$ patch and the ones tted when using a $30°$ patch. Modes in the l range of 100 to 200 are recovered with the larger area. We are particularly interested in these low-l modes for this study.

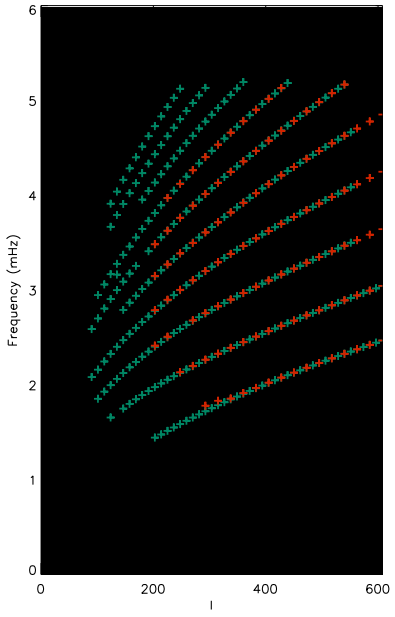

Figure 1. Comparison between the set of modes in the l range of 0 to 600 fitted using a $15°$ patch (red) and the ones fitted when using a $30°$ patch (green).

To verify the technique, we compare the rotation rate obtained with a traditional ring diagram analysis, the large-aperture approach, and the global helioseismic results for CR 1989 using both GONG and MDI full-disk Dopplergrams.

Fig. 2 shows the rotation rate for several latitudes ($0°$, $15°$, $30°$ and $45°$) from global analysis (Howe et al., 2000) and from ring diagrams analysis applied to GONG and MDI data. The local results are an average over CR 1989; the global ones span three months including that CR. There is a clear improvement in the results when the

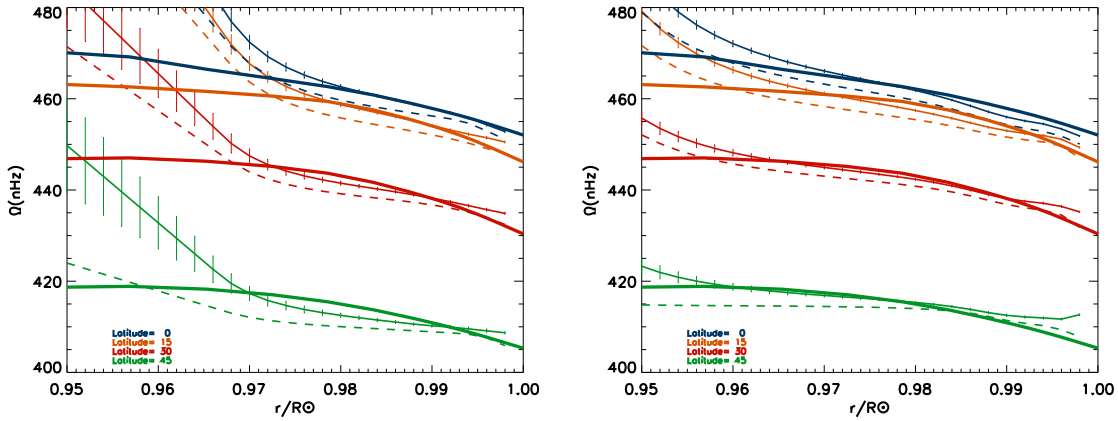

Figure 2. Rotation rate for several latitudes, $0°$*,* $15°$*,* $30°$ *and* $45°$ *from global analysis (thick solid line) and from ring diagrams (GONG solid line, MDI dashed line). The left panel shows the results obtained using the typical* $15°$ *patches, the right panel the same results using the larger* $30°$ *patches.*

larger areas are used. The systematic displacement between GONG and MDI results is still under investigation.

2. MERIDIONAL CIRCULATION VARIABILITY

We have studied six consecutive Carrington rotations 1987, 1988, 1989, 1990, 1991 and 1992 and averaged the results at each latitude for each of them. The data used for this work are GONG full-disk Dopplergrams. Fig. 3 shows the averaged meridional component of the horizontal velocity ows at different depths for these six rotations. We nd an equatorward ow in the northern hemisphere below $0.975 R_\odot$ for CRs 1987, 1988 and 1989. This ow has been seen in MDI data for the same period and was named the countercell (Haber et al., 2002). A southern hemisphere countercell appears for CR 1992. Fig. 4 presents the velocities resulting from combining the meridional component of the averaged horizontal velocity ows with the calculated vertical component. They have been calculated for CR 1988 using GONG data. The vertical component was derived using the continuity equation from the calculated divergence of the measured horizontal ows (Komm et al., 2004).

3. WHAT CAUSES THE COUNTERCELL?

In order to search for systematic errors in the meridional ows caused by geometrical effects, we analyzed CR 1979, CR 1988 and CR 1990 using GONG data. For these three CRs the B_0 solar angle is close to $+6.0°$, $-6.0°$ and $0°$ respectively. The comparisons shown in Fig. 5 look quite anti-symmetric for CR 1979 and CR 1988, revealing a northern hemisphere countercell for CR 1988, a southern hemisphere countercell for CR 1979 and no counter cell for CR 1990.

Finally, we look at three consecutive CRs using MDI full disk Dopplergrams: 1987, 1988 and 1989. Fig. 6 shows the meridional component of the horizontal velocity ows obtained for these three CRs. The B_0 angle during this period ranges from about $-7.5°$ for CR 1987 to approximately $-3.0°$ for CR 1989. It can be seen from the graphics that there is a marked correlation between the value of the B_0 angle and the progression of the countercell.

4. DISCUSSION

Large aperture ring diagrams prove to be effective in searching for differential rotation and meridional circulation in deeper layers under the solar surface. We will apply the technique to GONG continuous velocity data to search for a meridional circulation variation with the solar cycle. A previous study by Chou & Dai (2001) using TON data found variations that were different for the declining and the rising phase of Cycle 22. They also found a general increase with depth in the meridional ows of up to 40 m/s. Our work agrees with a slight increase in the magnitude of the meridional ows with depth; however, the major increase below $0.965 R_\odot$ is suspected to be an artifact of our inversion method and is under investigation.

Our preliminary results suggest that the presence of the countercell could be related to the B_0 angle. We suspect geometric calibration issues or the analysis method may affect the meridional circulation results.

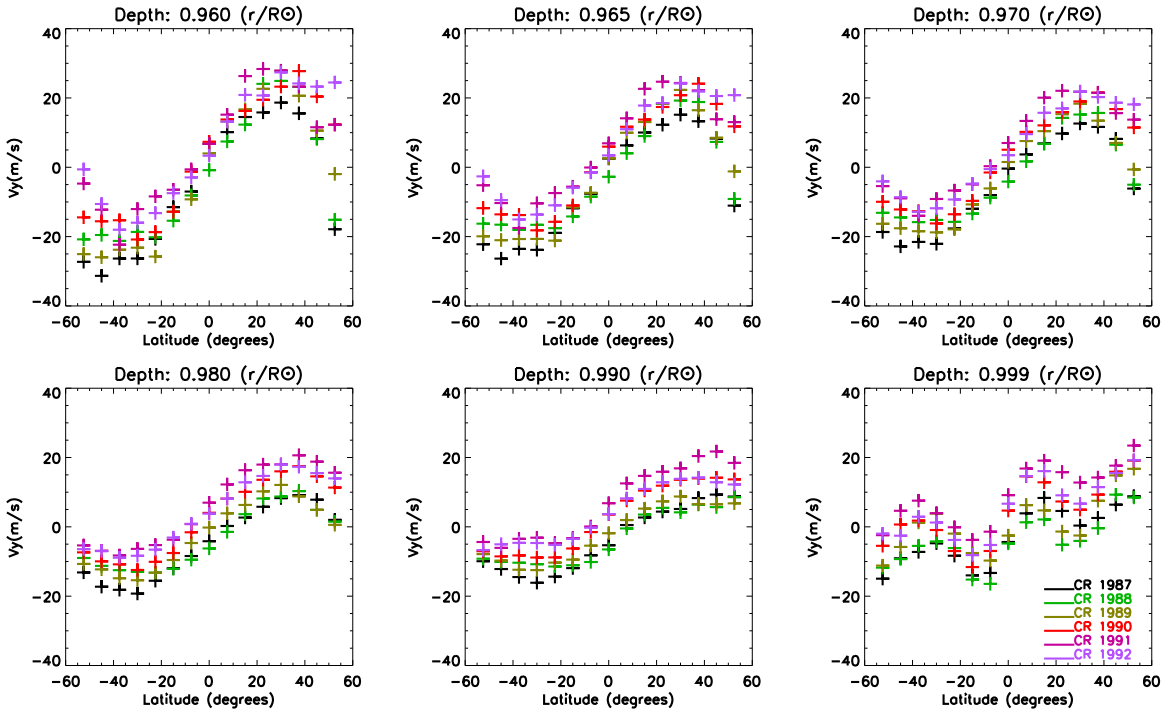

Figure 3. Meridional component of the horizontal velocity flows at six different depths for Carrington Rotations 1987, 1988, 1989, 1990, 1991 and 1992.

ACKNOWLEDGMENTS

We thank J. Bolding, R. Bogart, D. Haber, B. Hindman, R. Larsen and C. Toner for their contribution to the RD pipeline code. This work was supported by NASA grant NAG 5-11703. SOHO is a project of international cooperation between ESA and NASA. This work utilizes data obtained by the Global Oscillation Network Group (GONG) program, managed by the National Solar Observatory, which is operated by AURA, Inc. under a cooperative agreement with the National Science Foundation. The data were acquired by instruments operated by the Big Bear Solar Observatory, High Altitude Observatory, Learmonth Solar Observatory, Udaipur Solar Observatory, Instituto de Astrof·sica de Canarias, and Cerro Tololo Interamerican Observatory.

REFERENCES

Chou, D.Y. and Dai, D.C., 2001, ApJ 559, L175.

Corbard, T., Toner, C., Hill, F., Haber, D.,Bogart, R., Hindman, B., 2003, SOHO 12/GONG+ 2002: Local and Global Helioseismology: The Present and Future, ESA Publication Division, ESA-SP-517, 255.

Gonzalez Hernandez, I., Patrøn, J., Bogart, R.S. and the SOI Ring Diagram Team, 1999, ApJ 510, L153.

Haber, D.A., Hindman, B.W., Toomre, J., Bogart, R.S., Larsen, R.M. and Hill, F., 2002, ApJ 570, 255.

Hill, F., 1988, ApJ 333, 996.

Howe, R. et al, 2000, Science, 287, 2456

Komm, R., Corbard, T., Durney, B.R., Gonzalez Hernandez, I., Hill, F., Howe, R. and Toner, C., 2004, ApJ 605, 554.

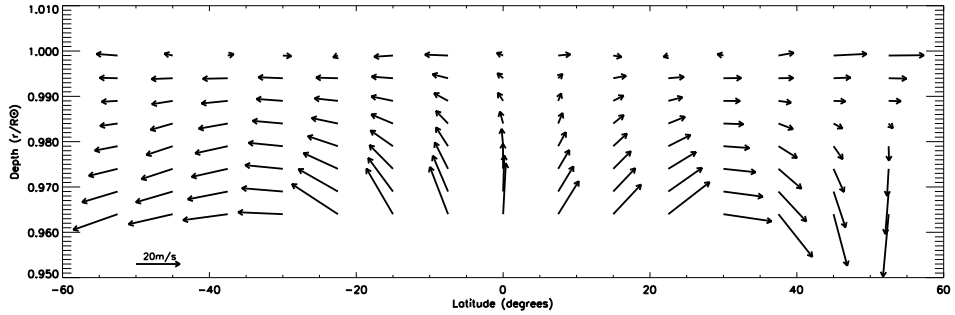

Figure 4. Velocity vectors obtained by combining the meridional component of the averaged horizontal velocity flows with the calculated vertical component. The data correspond to CR 1988.

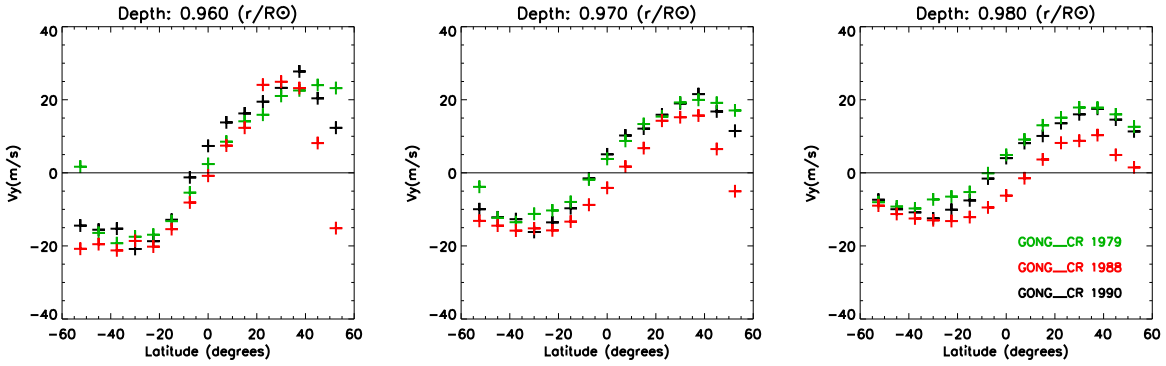

Figure 5. Meridional component of the horizontal velocity flows at three different depths. The data used are GONG full-disk dopplergrams and correspond to CRs 1979,1988 and 1990.

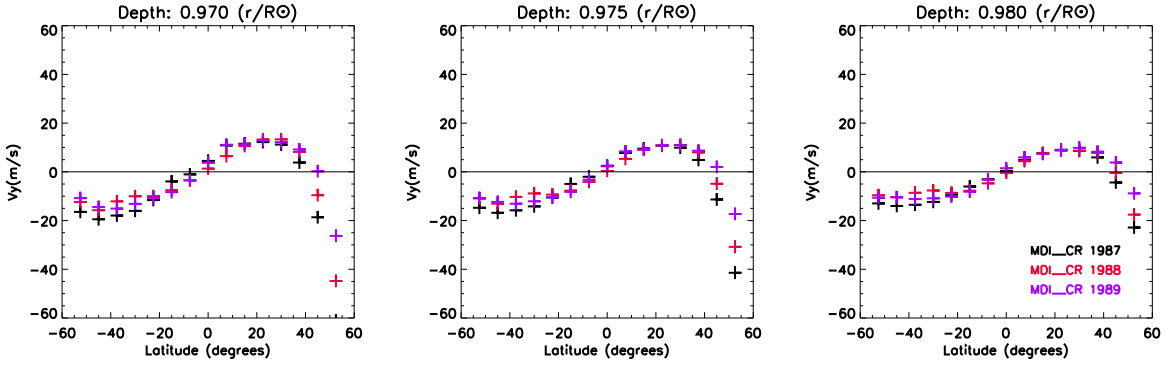

Figure 6. Meridional component of the horizontal velocity flows at three different depths. The data used are MDI full-disk dopplergrams and correspond to CRs 1987,1988 and 1989.